Simulation of gain in quantum cascade lasers

Wacker, Andreas; Nelander, Rikard; Weber, Carsten

Published in:
Proceedings of SPIE, the International Society for Optical Engineering

DOI:
10.1117/12.808882

2009

Simulation of gain in quantum cascade lasers

Andreas Wacker, Rikard Nelander, and Carsten Weber

Mathematical Physics, Lund University, Box 118, 22100 Lund, Sweden

ABSTRACT

The gain profile of a quantum cascade laser is strongly influenced by the lifetime of the carriers in the upper and lower laser state. The quantitative description of gain within the concept of nonequilibrium Green's functions allows for a detailed understanding of various features affecting the gain spectrum: Compensation effects between scattering processes in the upper and lower laser level, reduction of gain due to coherences between nearly degenerate upper laser states, and dispersive gain without inversion.

Keywords: Quantum Cascade Laser, linewidth, simulation

1. INTRODUCTION

Quantum cascade lasers (QCLs)[1] are semiconductor heterostructure lasers based on optical transitions between quantized intersubband levels in multiple quantum well structures. In these devices the inversion between the upper and lower laser level is achieved by selective tunneling processes at operating bias. They are now applied as sources both in the terahertz (THz) and mid-infrared regime.[2,3]

An important issue is the strength and line-width of the optical transition which determines the gain properties inside the optical cavity. Conventionally, one determines the eigenstates $\varphi_i(z)$ with energies E_i of the heterostructure under an applied bias together with the electron densities n_i.[4,5] Identifying the upper ($i = \mathrm{up}$) and lower laser level ($i = \mathrm{lo}$), Fermi's golden rule combined with level broadening provides the material gain:

$$G_{\mathrm{simple}}(\omega) = \frac{2e^2|z_{\mathrm{lo,up}}|^2\omega(n_{\mathrm{up}} - n_{\mathrm{lo}})}{dc\epsilon_0\sqrt{\epsilon_r}} \frac{\Gamma}{(E_{\mathrm{up}} - E_{\mathrm{lo}} - \hbar\omega)^2 + \Gamma^2/4} \tag{1}$$

where d is the period of the cascade structure, ϵ_r is the relative dielectric constant, and e the elementary charge. Γ is the full width at half maximum (FWHM) of the gain spectrum. Typically, one assumes that it is given by the sum of the scattering rates for both levels, i.e. $\Gamma = \Gamma_{\mathrm{up}} + \Gamma_{\mathrm{lo}}$. Here, Γ_i contains both the intersubband scattering processes, which redistribute carriers between the subbands, and intrasubband processes, which typically dominate. This provides four important issues for laser optimization by systematic design of the heterostructure: (i) Maximize the inversion $n_{\mathrm{up}} - n_{\mathrm{lo}}$, which is proportional to the gain, by strong injection of electrons from the injector into the upper laser state and efficient extraction from the lower state. (ii) Maximize the dipole element $z_{\mathrm{up,lo}}$ by employing a good wave function overlap between the upper and lower laser state. (iii) Reduce the intrasubband scattering in the active region in order to reduce Γ_{up} and Γ_{lo}. (iv) Minimize the laser period d. While these strategies are typically quite successful, there are some caveats which are discussed here, focusing on the physics beyond this simple approach.

In this context it is important which information is provided from the modeling of the electrical transport through the device. Standard rate equation models[5] provide the carrier densities n_i for each subband i and are fully sufficient for the use of Eq. (1). More detailed Monte-Carlo schemes[6] provide the occupation functions $f_i(\mathbf{k})$ for the electronic states with wave-vector $\mathbf{k}$ in the direction parallel to the layers. The gain can be evaluated in analogy to Eq. (1); however, gain without inversion is possible if the dipole matrix element is strongly $\mathbf{k}$-dependent and/or there is a strong nonparabolicity.[7,8] Correlations between the states $\rho_{ij}(\mathbf{k})$ can be treated by density matrix schemes[6,9–11] which allow for a quantitative analysis of tunneling close to level crossings between the injector ground state and the upper laser level.[12,13] In this context, gain without inversion is possible as well.[14] Finally, the energetically resolved density matrix, the Green's function $G^<_{ij}(\mathbf{k}, E)$ provides a detailed description of broadening effects. It can be determined self-consistently within the concept of nonequilibrium Green's functions (NEGF)[15,16] for the QCL.

Send correspondence to A.W.: E-mail: Andreas.Wacker@fysik.lu.se

Novel In-Plane Semiconductor Lasers VIII, edited by Alexey A. Belyanin, Peter M. Smowton,
Proc. of SPIE Vol. 7230, 72301A · © 2009 SPIE · CCC code: 0277-786X/09/$18 · doi: 10.1117/12.808882

2. DISPERSIVE GAIN

The NEGF model sketched in the Appendix provides the following expression for the gain, if we restrict to the upper and lower laser level as well as diagonal parts of the stationary Green's functions and neglect counter rotating terms:

$$G_{\text{two level}}(\omega) = \frac{e^2(E_{\text{up}}-E_{\text{lo}})|z_{\text{lo,up}}|^2}{2cd\hbar\epsilon_0\sqrt{\epsilon_r}}\frac{2}{A}\sum_{\mathbf{k}}\int\frac{\mathrm{d}E}{2\pi} \Big[\Im\{G^<_{\text{up,up}}(\mathbf{k},E+\hbar\omega)\}A_{\text{lo}}(\mathbf{k},E) - A_{\text{up}}(\mathbf{k},E+\hbar\omega)\Im\{G^<_{\text{lo,lo}}(\mathbf{k},E)\}\Big] \tag{2}$$

where A is the cross section. Here $A_i(\mathbf{k},E)$ is the spectral function of the level, which is frequently assumed to have the generic Lorentzian shape

$$A_i(\mathbf{k},E) \approx \frac{\Gamma_i}{(E-E_i(\mathbf{k}))^2+\Gamma_i^2/4}$$

The lesser Green's function provides the occupation of the levels and its diagonal elements can be parameterized as

$$G^<_{ii}(\mathbf{k},E) = \mathrm{i}f_i(\mathbf{k},E)A_i(\mathbf{k},E)\,,$$

where $0 \le f_i(\mathbf{k},E) \le 1$ is a generalized level occupation. If we assume (i) the Lorentzian approximation of the spectral functions, (ii) that $f_i(\mathbf{k},E) = f_i(\mathbf{k})$ does not depend on E, and (iii) parabolic bands with $E_i(\mathbf{k}) = E_i + \hbar^2k^2/2m^*$ (with effective mass m^*), we obtain Eq. (1) with $\Gamma = \Gamma_{\text{up}} + \Gamma_{\text{lo}}$. Here we also used

$$n_i = \frac{2(\text{for spin})}{A}\sum_{\mathbf{k}} f_i(\mathbf{k}) \tag{3}$$

and replaced $E_{\text{up}} - E_{\text{lo}}$ by $\hbar\omega$, which holds at resonance.

This situation is sketched in Fig. 1(c), where the spectral functions of the upper and lower level are depicted for a given k. The arrows depict transitions at a given frequency ω, and gain is found in a frequency region $|\hbar\omega - (E_{\text{up}} - E_{\text{lo}})| \lesssim \Gamma$, provided the occupation $f_i(\mathbf{k})$ (grey-scale) is larger for the upper laser level.

However, this only holds if $f_i(\mathbf{k},E) = f_i(\mathbf{k})$ is constant on the energy scale of Γ_i. Otherwise, $f_i(\mathbf{k},E)$ is typically decreasing in energy due to coupling to a local energy bath. This situation is depicted in Fig. 1(e), where equal total populations $\int \mathrm{d}E f_i(\mathbf{k},E)A_i(\mathbf{k},E) = 2\pi f_i(\mathbf{k})$ are assumed. As shown by the transition arrows, Eq. (2) provides a dispersive structure of the gain, see Fig. 1(f), as recently observed in QCLs.[18,19] The same effect is common for superlattices where the total occupation $f_i(\mathbf{k})$ is identical for all Wannier-Stark states belonging to the lowest miniband.[20]

3. REDUCED WIDTH OF GAIN PEAK BY CORRELATED SCATTERING

In the derivation of Eq. (2), we restricted to the first line in Eq. (27) which is not always appropriate. As shown in Ref. 21, inclusion of the term $\delta\Sigma^<$ for elastic scattering provides again Eq. (1) with an effective FWHM

$$\Gamma_{\text{eff}}(\mathbf{k}) = \Gamma_{\text{up}}(\mathbf{k}) + \Gamma_{\text{lo}}(\mathbf{k}) - 2\frac{Am^*}{\hbar^2}\sum_{\mathbf{k}'}\langle V^{\text{elast}}_{\text{up,up}}(\mathbf{k}-\mathbf{k}')V^{\text{elast}}_{\text{lo,lo}}(\mathbf{k}'-\mathbf{k})\rangle \tag{4}$$

This result has been obtained earlier[22] as well and shows that the choice $\Gamma = \Gamma_{\text{up}} + \Gamma_{\text{lo}}$ can overestimate the linewidth.

In Fig. 2 (left panel), the gain calculated by our full NEGF model (see appendix) is shown for the QCL of Ref. 23 by the red solid line. For comparison, the gain is evaluated by an extension of Eq. (1) taking into account all possible transitions. Here the same densities and scattering parameters are used as for the NEGF result. The choice $\Gamma = \Gamma_{\text{up}} + \Gamma_{\text{lo}}$ (blue dotted line) provides a far too large line-width in accordance with the discussion above. In contrast, the use of Eq. (4) overestimates the compensation effect, see the green dashed line.

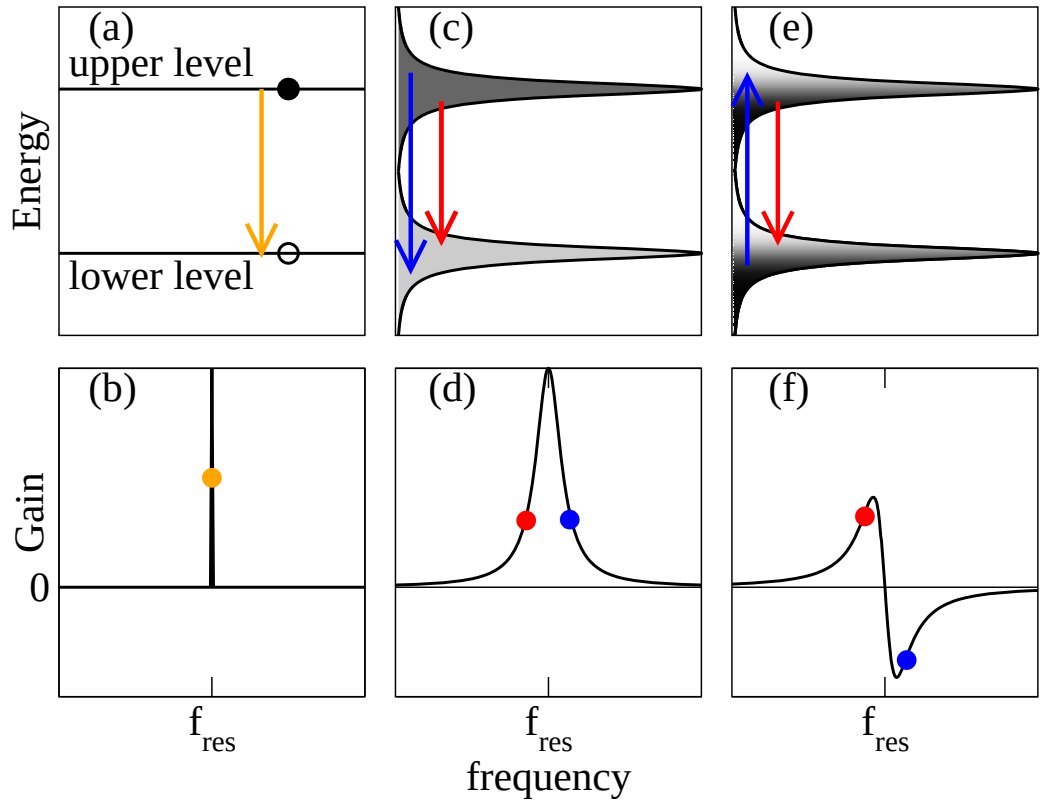

Figure 1. Density of states combined with occupation probability in grey-scale (upper panel) and gain spectrum (lower panel) for different levels of description for the gain in a two level system: (a,b) two pure levels, (c,d) broadened levels, and (e,f) broadened levels with energy-dependent occupations $f(\mathbf{k}, E)$. See also Ref. 17.

Furthermore, there is a red shift in the gain peak comparing the NEGF result with Eq. (1). This is a sign of the dispersive gain, see also Ref. 24, as demonstrated in the right panel of Fig. 2. The calculation of Eq. (1) provides a gain peak at the energy difference between the maxima of the spectral functions which are taken as effective level energies. In contrast, the lesser Green's function $G^{<}_{\mathrm{up,up}}(\mathbf{k}, E)$ does not follow $A_{\mathrm{up}}(\mathbf{k}, E)$ but has a peak at lower energies. This corresponds to an energy dependence of the effective occupation $f_i(\mathbf{k}, E)$ as discussed in Sec. 2. Correspondingly, the gain is enhanced for frequencies below $E_{\mathrm{up}} - E_{\mathrm{lo}}$ and decreased above, which leads to the red shift observed.

4. REDUCTION OF GAIN BY COHERENCE ACROSS THE INJECTION BARRIER

A third issue is the interference with other levels. In this context, the ground state of the injector (denoted by in) is of relevance. Its energy E_{in} is close to the energy of the upper laser state E_{up}, ensuring a fast charge transfer to the upper laser level. While such coherences are fully treated within our Green's function approach, they have been neglected during the derivation of Eq. (2) and consequently also for Eq. (1). Here we give a simplified description within density matrix theory in order to demonstrate their relevance.

The semiconductor Bloch equations[26] for this three level system read

$$\begin{aligned} \mathrm{i}\hbar\dot{\rho}_{\mathrm{up,lo}}(\mathbf{k},t) &= (E_{\mathrm{up}} - E_{\mathrm{lo}} - \mathrm{i}\Gamma_{\mathrm{up,lo}}(\mathbf{k})/2)\,\rho_{\mathrm{up,lo}}(\mathbf{k},t) \\ &\quad -eF(t)\left\{z_{\mathrm{in,lo}}\rho_{\mathrm{up,in}}(\mathbf{k},t) - z_{\mathrm{up,in}}\rho_{\mathrm{in,lo}}(\mathbf{k},t) + z_{\mathrm{up,lo}}\left[f_{\mathrm{up}}(\mathbf{k},t) - f_{\mathrm{lo}}(\mathbf{k},t)\right]\right\}, \qquad (5) \\ \mathrm{i}\hbar\dot{\rho}_{\mathrm{in,lo}}(\mathbf{k},t) &= (E_{\mathrm{in}} - E_{\mathrm{lo}} - \mathrm{i}\Gamma_{\mathrm{in,lo}}(\mathbf{k})/2)\,\rho_{\mathrm{in,lo}}(\mathbf{k},t) \\ &\quad -eF(t)\left\{z_{\mathrm{up,lo}}\rho_{\mathrm{in,up}}(\mathbf{k},t) - z_{\mathrm{in,up}}\rho_{\mathrm{up,lo}}(\mathbf{k},t) + z_{\mathrm{in,lo}}\left[f_{\mathrm{in}}(\mathbf{k},t) - f_{\mathrm{lo}}(\mathbf{k},t)\right]\right\}, \qquad (6) \end{aligned}$$

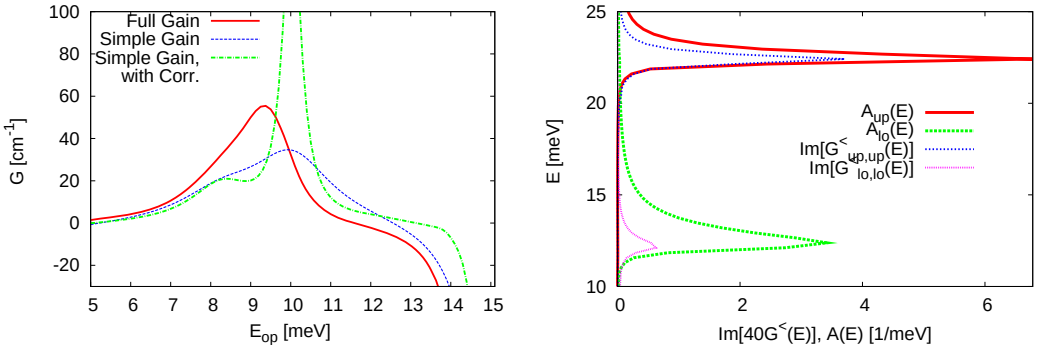

Figure 2. Left: Gain spectrum calculated by the NEGF model at a bias of 46.5 mV per period for the laser of Ref. 23 at 20 K. For calculation details, see Ref. 25. Right: Spectral function $A_i(\mathbf{k}, E)$ and lesser Green's function $\Im\{G^<_{ii}(\mathbf{k}, E)\}$ for the upper and lower laser level extracted for the same operation point.

where $F(t)$ is the optical field. Now we assume that in the stationary state all nondiagonal density matrices are vanishing small except for $\rho_{\mathrm{in,up}}(k)$, which describes the stationary coherence related to the tunneling processes across the injection barrier.[12,13,16] Within linear response, the electrical polarization is given by

$$P(t) = -\frac{2e}{Ad}\sum_{\mathbf{k}}\left[z_{\mathrm{lo,up}}\rho_{\mathrm{up,lo}}(\mathbf{k},t) + z_{\mathrm{lo,in}}\rho_{\mathrm{in,lo}}(\mathbf{k},t)\right] + h.c. \tag{7}$$

After Fourier transformation and neglecting counter-rotating terms we obtain the gain

$$\begin{aligned} G(\omega) =& -\frac{\omega}{\sqrt{\epsilon_r}\epsilon_0 c}\Im\left\{\frac{P(\omega)}{F(\omega)}\right\} \\ =& \frac{\omega e^2}{2\sqrt{\epsilon_r}\epsilon_0 c}\frac{2}{Ad}\sum_{\mathbf{k}}\left\{\frac{\Gamma_{\mathrm{up,lo}}(\mathbf{k})\left[|z_{\mathrm{up,lo}}|^2\left(f_{\mathrm{up}}(\mathrm{k}) - f_{\mathrm{lo}}(\mathrm{k})\right) + \Re\{z_{\mathrm{lo,up}}z_{\mathrm{in,lo}}\rho_{\mathrm{up,in}}(\mathrm{k})\}\right]}{(E_{\mathrm{up}} - E_{\mathrm{lo}} - \hbar\omega)^2 + \Gamma^2_{\mathrm{up,lo}}(\mathbf{k})/4}\right. \\ &\left. + \frac{\Gamma_{\mathrm{in,lo}}(\mathbf{k})\left[|z_{\mathrm{in,lo}}|^2\left(f_{\mathrm{in}}(\mathrm{k}) - f_{\mathrm{lo}}(\mathrm{k})\right) + \Re\{z_{\mathrm{lo,in}}z_{\mathrm{up,lo}}\rho_{\mathrm{in,up}}(\mathrm{k})\}\right]}{(E_{\mathrm{in}} - E_{\mathrm{lo}} - \hbar\omega)^2 + \Gamma^2_{\mathrm{in,lo}}(\mathbf{k})/4}\right\} \end{aligned} \tag{8}$$

If the contribution of the injector state is negligible, this reproduces Eq. (1). On the other hand, at an ideal level crossing, $E_{\mathrm{in}} \approx E_{\mathrm{up}}$ and $\varphi_{\mathrm{up/in}}(z) = [\varphi_{\mathrm{left}}(z) \pm \varphi_{\mathrm{right}}(z)]/\sqrt{2}$, where $\varphi_{\mathrm{left/right}}(z)$ are localized on the left/right-hand side of the injection barrier. This implies $z_{\mathrm{lo,up}} \approx -z_{\mathrm{lo,in}}$ and $\Gamma_{up,lo} \approx \Gamma_{in,lo}$ and we obtain:

$$G(\omega) = \frac{\omega e^2|z_{\mathrm{up,lo}}|^2}{2\sqrt{\epsilon_r}\epsilon_0 c}\frac{2}{Ad}\sum_{\mathbf{k}}\frac{\Gamma_{\mathrm{up,lo}}(\mathbf{k})}{(E_{\mathrm{up}} - E_{\mathrm{lo}} - \hbar\omega)^2 + \Gamma^2_{\mathrm{lo,up}}(\mathbf{k})/4}\left[f_{\mathrm{up}}(\mathrm{k}) + f_{\mathrm{in}}(\mathrm{k}) - 2f_{\mathrm{lo}}(\mathrm{k}) - 2\Re\{\rho_{\mathrm{in,up}}(\mathrm{k})\}\right] \tag{9}$$

Thus, the gain is reduced by the presence of coherence between the injector and upper laser level. This becomes pronounced for thicker injection barriers, where the strong coherence $\rho_{\mathrm{in,up}}(\mathrm{k}) \approx f_{\mathrm{up}}(\mathrm{k}) \approx f_{\mathrm{in}}(\mathrm{k})$ shows that the delocalized eigenstates do not satisfactorily represent the carrier distribution, which is localized on the left-hand side of the injection barrier. As an example, this effect is demonstrated within our density matrix model[13] for the QCL structure of Fig. 3(left), where we consider different widths of the injection barrier b. While the carrier occupations do not change much with the width of the injector barrier under resonance conditions (right part of Fig. 3), the gain is strongly suppressed for a thick injection barrier and even vanishes albeit the occupations of the upper laser level and the injector level remain large (Fig. 4).

5. CONCLUSION

While an estimate of the gain peak by the Lorentzian approximation (1) is often helpful for a simple analysis, there are several features not contained in this pictures. Dispersive gain can provide an effective red shift of

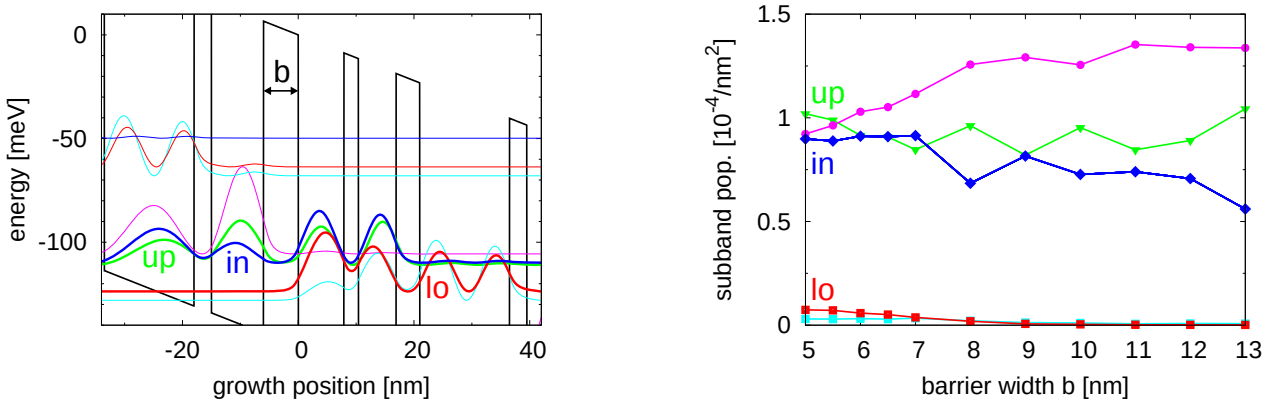

Figure 3. Left: QCL structure of Ref. 27, which we study for different injection barrier widths b (here: $b = 6.0$ nm). Right: Occupation of energy eigenstates as a function of barrier width under resonance condition. The calculations are performed by the density matrix model of Ref. 13.

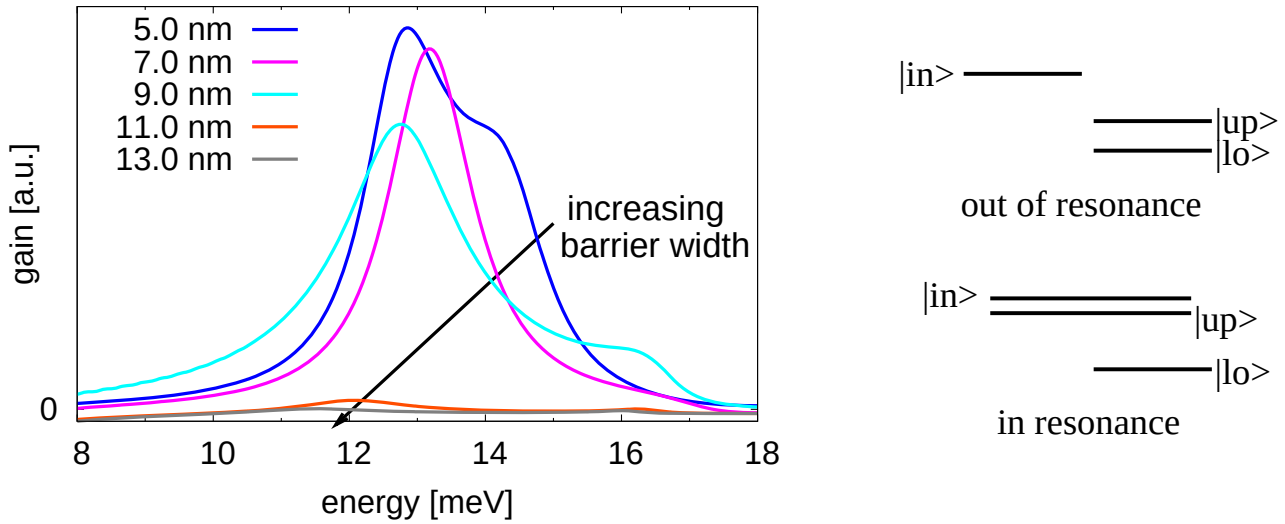

Figure 4. Left: Calculated gain spectrum for the sample of Fig. 3 for different thicknesses of the injection barrier under resonance condition. Right: Sketch of the relevant levels and coherence: Top: out of resonance, bottom: under resonance condition between the upper laser level and the injector level.

the gain peak and yield gain when no population inversion is present. The width of the gain peak is generally overestimated if one simply adds the scattering rates of the upper and lower laser level. Furthermore, coherent superpositions of eigenstates can lead to strong modifications in the gain spectrum. All these features are fully contained in a simulation by nonequilibrium Green's functions.

APPENDIX A. FULL THEORY BY GREEN FUNCTIONS

Within our Green's function approach, we consider a Hamiltonian

$$\hat{H} = \underbrace{\sum_{\alpha,\beta,\mathbf{k}} U_{\alpha,\beta}(\mathbf{k}) a^\dagger_\alpha(\mathbf{k}) a_\beta(\mathbf{k})}_{\hat{H}_0} + \hat{H}_{\text{scatt}} \tag{10}$$

where the indices α, β denote a set of orthonormal basis states $\Psi_\alpha(z)$ together with plane waves $\mathrm{e}^{\mathrm{i}(k_x x + k_y y)}/\sqrt{A}$. $\hat{H}_{\text{scatt}}$ contains, in contrast to $\hat{H}_0$, elements which are nondiagonal in $\mathbf{k}$, i.e. break the translational invariance. This term will be treated perturbatively using self-energies Σ. We assume

$$U_{\alpha\beta}(\mathbf{k}) = U_{\alpha\beta} + E_k \delta_{\alpha\beta}$$

where $E_k = \hbar^2 k^2 / 2m^*$ is the corresponding lateral kinetic energy, assuming a constant effective mass m^* in the in-plane direction (neglecting non-parabolicity and non-separability). $U_{\alpha,\beta}$ contains the kinetic energy, the heterostructure potential and the electrical potential due to a constant external field F (in z-direction).

We apply the formalism of nonequilibrium Green's functions[28] and define the correlation function (or 'lesser' Green's function)

$$G^<_{\alpha_1,\alpha_2}(\mathbf{k}; t_1, t_2) = \mathrm{i} \langle \hat{a}^\dagger_{\alpha_2}(\mathbf{k}, t_2) \hat{a}_{\alpha_1}(\mathbf{k}, t_1) \rangle \tag{11}$$

and the retarded and advanced Green's functions

$$G^{\text{ret}}_{\alpha_1,\alpha_2}(\mathbf{k}; t_1, t_2) = -\mathrm{i}\Theta(t_1 - t_2) \langle \left\{ \hat{a}_{\alpha_1}(\mathbf{k}, t_1), \hat{a}^\dagger_{\alpha_2}(\mathbf{k}, t_2) \right\} \rangle \tag{12}$$

$$G^{\text{adv}}_{\alpha_1,\alpha_2}(\mathbf{k}; t_1, t_2) = \mathrm{i}\Theta(t_2 - t_1) \langle \left\{ \hat{a}_{\alpha_1}(\mathbf{k}, t_1), \hat{a}^\dagger_{\alpha_2}(\mathbf{k}, t_2) \right\} \rangle = \left[G^{\text{ret}}_{\alpha_2,\alpha_1}(\mathbf{k}, t_2, t_1) \right]^* \tag{13}$$

respectively, where $\{\hat{a}, \hat{b}\} = \hat{a}\hat{b} + \hat{b}\hat{a}$ denotes the anti-commutator which is appropriate for fermion operators a_α considered here.

A.1 Stationary state and transport

We consider a stationary state without any time dependence of the external potential. Then, all functions depend only on the time difference $t_1 - t_2$, and it is convenient to work in Fourier space defined by

$$F_{\alpha_1,\alpha_2}(\mathbf{k}, E) = \frac{1}{\hbar} \int \mathrm{d}t \, \mathrm{e}^{\mathrm{i}Et/\hbar} F_{\alpha_1,\alpha_2}(\mathbf{k}; t + t_2, t_2) \tag{14}$$

$$F_{\alpha_1,\alpha_2}(\mathbf{k}; t_1, t_2) = \frac{1}{2\pi} \int \mathrm{d}E \, \mathrm{e}^{-\mathrm{i}E(t_1 - t_2)/\hbar} F_{\alpha_1,\alpha_2}(\mathbf{k}, E) \tag{15}$$

both for the self-energies and the Green's functions. Then one obtains the following matrix equations for the Green's functions, see also chapter 4 of Ref. 29: The *Dyson equation*

$$E G^{\text{ret/adv}}_{\alpha_1,\alpha_2}(\mathbf{k}, E) - \sum_\beta \left(U_{\alpha_1,\beta}(\mathbf{k}) + \Sigma^{\text{ret/adv}}_{\alpha_1,\beta}(\mathbf{k}, E) \right) G^{\text{ret/adv}}_{\beta,\alpha_2}(\mathbf{k}, E) = \delta_{\alpha_1,\alpha_2} \tag{16}$$

and the *Keldysh relation*

$$G^<_{\alpha_1,\alpha_2}(\mathbf{k}, E) = \sum_{\beta,\beta'} G^{\text{ret}}_{\alpha_1,\beta}(\mathbf{k}, E) \Sigma^<_{\beta,\beta'}(\mathbf{k}, E) G^{\text{adv}}_{\beta',\alpha_2}(\mathbf{k}, E) \,. \tag{17}$$

The lesser Green's function is related to the density matrix via

$$\rho_{\alpha\beta}(\mathbf{k},t) = \langle \hat{a}^\dagger_\beta(\mathbf{k},t)\hat{a}_\alpha(\mathbf{k},t)\rangle = -\mathrm{i}\int \frac{\mathrm{d}E}{2\pi}\, G^<_{\alpha,\beta}(\mathbf{k},E) \tag{18}$$

so that it can be viewed as an energy-resolved density matrix. The electron charge density can be evaluated by

$$\rho_{\mathrm{el}}(z) = \frac{-2(\text{for Spin})e}{A}\sum_{\alpha\beta}\sum_{k}\rho_{\alpha\beta}(\mathbf{k})\Psi^*_\beta(z)\Psi_\alpha(z) \tag{19}$$

The mean field potential $\phi^{\mathrm{MF}}(z)$ is obtained from the Poisson equation taking into account the doping density and the electron density together with periodic boundary conditions $\phi^{\mathrm{MF}}(z+d) = \phi^{\mathrm{MF}}(z)$. This mean field potential induces a new part in the Hamiltonian with matrix elements

$$U^{\mathrm{MF}}_{\alpha\beta} = -e\int \mathrm{d}z \Psi^*_\alpha(z)\phi^{\mathrm{MF}}(z)\Psi_\beta(z)\,. \tag{20}$$

The current is evaluated by considering the temporal evolution of $\langle\hat{z}\rangle$, providing

$$J = -\frac{e}{V}\langle\dot{z}\rangle = \underbrace{-\frac{e}{V}\left\langle\frac{\mathrm{i}}{\hbar}[\hat{H}_0,\hat{z}]\right\rangle}_{=J_0}\underbrace{-\frac{e}{V}\left\langle\frac{\mathrm{i}}{\hbar}[\hat{H}_{\mathrm{scatt}},\hat{z}]\right\rangle}_{=J_{\mathrm{scatt}}}, \tag{21}$$

where the scattering current vanishes, if one takes into account the full matrix structure of the self-energies[16] in contrast to earlier work.[15] For an arbitrary choice of the basis, we may write

$$J_0(t) = \frac{-2(\text{for Spin})e}{V}\frac{\mathrm{i}}{\hbar}\sum_{\mathbf{k}}\sum_{\beta\alpha}W_{\beta,\alpha}\rho_{\alpha\beta}(\mathbf{k},t) \quad \text{where} \quad W_{\beta,\alpha} = \sum_\gamma U_{\beta\gamma}z_{\gamma\alpha} - z_{\beta\gamma}U_{\gamma\alpha}\,. \tag{22}$$

The approximations occur in the evaluation of the self-energies, where we apply the self-consistent Born approximation, which reads for elastic scattering processes

$$\Sigma^{</\mathrm{ret}}_{\alpha\alpha'}(\mathbf{k},E) = \sum_{\beta\beta'}\sum_{\mathbf{k}'}\langle V^{\mathrm{elast}}_{\alpha\beta}(\mathbf{k}-\mathbf{k}')V^{\mathrm{elast}}_{\beta'\alpha'}(\mathbf{k}'-\mathbf{k})\rangle G^{</\mathrm{ret}}_{\beta\beta'}(\mathbf{k}',E) \tag{23}$$

In order to reduce the computational demand, we use a constant scattering matrix element providing self-energies which do not depend on $\mathbf{k}$ in our numerical calculations. The phonon self-energies have a similar matrix structure, but couple between different energies, see Refs. 15, 29 for details. Our program iteratively solves Eqs. (16,17) and Eq. (23) together with the phonon self-energies until self-consistency is reached and the current is calculated by Eq. (22).

A.2 Gain

Now we consider the additional potentials due to a time-dependent electric field

$$\delta U_{\alpha\beta}(t) = \int\frac{\mathrm{d}\omega}{2\pi}e\delta F(\omega)z_{\alpha\beta}\mathrm{e}^{-\mathrm{i}\omega t} \tag{24}$$

which describes the optical field in the dipole approximation.

Due to the time dependence of the external field, the Green's functions $\delta G(t_1,t_2)$ exhibit an explicit time dependence in both arguments. This two-time structure is fully taken into account by applying the Fourier decomposition in both times via

$$\delta\mathbf{G}(\mathbf{k},t_1,t_2) = \int\frac{\mathrm{d}\omega}{2\pi}\mathrm{e}^{-\mathrm{i}\omega t_1}\int\frac{\mathrm{d}E}{2\pi}\delta\mathbf{G}(\mathbf{k},\omega,E)\mathbf{k},\mathrm{e}^{-\mathrm{i}E(t_1-t_2)/\hbar}\,. \tag{25}$$

The same decomposition is used for $\delta\Sigma$. Then we find within linear response:[20]

$$\delta\mathbf{G}^{\mathrm{ret/adv}}(\mathbf{k},\omega,E) = \tilde{\mathbf{G}}^{\mathrm{ret/adv}}(\mathbf{k},E+\hbar\omega)\left[\delta\mathbf{U}(\omega)+\delta\mathbf{\Sigma}^{\mathrm{ret/adv}}(\mathbf{k},\omega,E)\right]\tilde{\mathbf{G}}^{\mathrm{ret/adv}}(\mathbf{k},E) \tag{26}$$

$$\begin{aligned}\delta\mathbf{G}^{<}(\mathbf{k},\omega,E) = {} & \tilde{\mathbf{G}}^{\mathrm{ret}}(\mathbf{k},E+\hbar\omega)\delta\mathbf{U}(\omega)\tilde{\mathbf{G}}^{<}(\mathbf{k},E)+\tilde{\mathbf{G}}^{<}(\mathbf{k},E+\hbar\omega)\delta\mathbf{U}(\omega)\tilde{\mathbf{G}}^{\mathrm{adv}}(\mathbf{k},E)\\ & +\tilde{\mathbf{G}}^{\mathrm{ret}}(\mathbf{k},E+\hbar\omega)\delta\mathbf{\Sigma}^{\mathrm{ret}}(\mathbf{k},\omega,E)\tilde{\mathbf{G}}^{<}(\mathbf{k},E)+\tilde{\mathbf{G}}^{\mathrm{ret}}(\mathbf{k},E+\hbar\omega)\delta\mathbf{\Sigma}^{<}(\mathbf{k},\omega,E)\tilde{\mathbf{G}}^{\mathrm{adv}}(\mathbf{k},E)\\ & +\tilde{\mathbf{G}}^{<}(\mathbf{k},E+\hbar\omega)\delta\mathbf{\Sigma}^{\mathrm{adv}}(\mathbf{k},\omega,E)\tilde{\mathbf{G}}^{\mathrm{adv}}(\mathbf{k},E)\,,\end{aligned} \tag{27}$$

where $\tilde{\mathbf{G}}$ denotes the stationary Green's functions of the self-consistent calculations described above. The changes in the self-energies $\delta\Sigma(\mathbf{k},\omega,E)=\mathcal{F}_E\{\delta G^{\mathrm{ret}}(\mathbf{k},\omega,E'),\delta G^{<}(\mathbf{k},\omega,E')\}$ are given by the same functionals as the self-energies $\Sigma(\mathbf{k},E)=\mathcal{F}_E\{G^{\mathrm{ret}}(\mathbf{k},E'),G^{<}(\mathbf{k},E')\}$ within the Born approximation, which is linear in G. They have to be determined self-consistently with the functions δG, which requires an additional iterative loop.

In addition to the scattering processes, the change in the mean-field δU^{MF} can also be taken into account. This is just the Hartree term of the self-energy

$$\delta\Sigma^{\mathrm{ret}}(\omega,E)=\delta\Sigma^{\mathrm{adv}}(\omega,E)=\delta U^{\mathrm{MF}}(\omega)\quad\text{and}\,\delta\Sigma^{<}(\omega,E)=0$$

The physical meaning of δU^{MF} is the depolarization shift. $\delta U^{\mathrm{MF}}(\omega)$ is determined in analogy to the stationary mean field potential.

The current is evaluated in linear response from Eq. (22), yielding

$$\delta J_0(\omega)=-\frac{2e}{V}\frac{\mathrm{i}}{\hbar}\sum_{\mathbf{k}}\sum_{\beta\alpha}W_{\beta,\alpha}\delta\rho_{\alpha\beta}(\mathbf{k},\omega) \tag{28}$$

where

$$\delta\rho_{\alpha\beta}(\mathbf{k},\omega)=-\mathrm{i}\int\frac{\mathrm{d}E}{2\pi}\,\delta G^{<}_{\alpha,\beta}(\mathbf{k},\omega,E) \tag{29}$$

The complex conductivity reads $\sigma(\omega)=\frac{\delta\langle J_0\rangle(\omega)}{\delta F(\omega)}$ and the material gain is finally given by

$$G(\omega)=-\frac{\Re\{\sigma(\omega)\}}{c\epsilon_0\sqrt{\epsilon_r}}$$

which is the main result and used for our numerical calculations.

If we consider energy eigenstates α and restrict to the upper and lower laser level in Eq. (28), we obtain

$$G(\omega)=\frac{2e}{cAd\hbar\epsilon_0\sqrt{\epsilon_r}\delta F(\omega)}\sum_{\mathbf{k}}\Re\left\{\mathrm{i}W_{\mathrm{lo,up}}\delta\rho_{\mathrm{up,lo}}(\mathbf{k},\omega)+\mathrm{i}W_{\mathrm{up,lo}}\delta\rho_{\mathrm{lo,up}}(\mathbf{k},\omega)\right\}\,.$$

Restricting to the first line in (27) and assuming diagonal stationary Green's functions $\tilde{\mathbf{G}}$, the $\delta\rho_{\mathrm{up,lo}}$ term provides

$$G(\omega)=\frac{e^2(E_{\mathrm{lo}}-E_{\mathrm{up}})|z_{\mathrm{lo,up}}|^2}{cd\hbar\epsilon_0\sqrt{\epsilon_r}}\frac{2}{A}\sum_{\mathbf{k}}\int\frac{\mathrm{d}E}{2\pi}\Re\left\{\tilde{G}^{\mathrm{ret}}_{\mathrm{up,up}}(\mathbf{k},E+\hbar\omega)\tilde{G}^{<}_{\mathrm{lo,lo}}(\mathbf{k},E)+\tilde{G}^{<}_{\mathrm{up,up}}(\mathbf{k},E+\hbar\omega)\tilde{G}^{\mathrm{adv}}_{\mathrm{lo,lo}}(\mathbf{k},E)\right\}$$

The $\delta\rho_{\mathrm{lo,up}}$ term has a corresponding structure, but here the peaks of $\tilde{G}^{\mathrm{ret}}_{\mathrm{lo,lo}}(\mathbf{k},E+\hbar\omega)$ and $\tilde{G}^{<}_{\mathrm{up,up}}(\mathbf{k},E)$ coincide only for negative frequencies (counter rotating terms). Neglecting this part and using $\Re\{\tilde{G}^{<}_{\alpha,\alpha}(\mathbf{k},E)\}=0$ and the spectral function $A_\alpha(\mathbf{k},E)=\mp2\Im\{\tilde{G}^{\mathrm{ret/adv}}_{\alpha,\alpha}(\mathbf{k},E)\}$, we find Eq. (2).

ACKNOWLEDGMENTS

Financial Support by the Swedish Science Foundation (VR) is gratefully acknowledged.

REFERENCES

[1] Faist, J., Capasso, F., Sivco, D. L., Sirtori, C., Hutchinson, A. L., and Cho, A. Y., "Quantum cascade laser," *Science* **264**, 553 (1994).

[2] Gmachl, C., Capasso, F., Sivco, D. L., and Cho, A. Y., "Recent progress in quantum cascade lasers and applications," *Rep. Prog. Phys.* **64**, 1533 (2001).

[3] Lee, M. and Wanke, M. C., "APPLIED PHYSICS: Searching for a Solid-State Terahertz Technology," *Science* **316**, 64 (2007).

[4] Capasso, F., Faist, J., and Sirtori, C., "Mesoscopic phenomena in semiconductor nanostructures by quantum design," *J. Math. Phys.* **37**, 4775 (1996).

[5] Indjin, D., Harrison, P., Kelsall, R. W., and Ikonic, Z., "Self-consistent scattering theory of transport and output characteristics of quantum cascade lasers," *J. Appl. Phys.* **91**, 9019 (2002).

[6] Iotti, R. C. and Rossi, F., "Nature of charge transport in quantum-cascade lasers," *Phys. Rev. Lett.* **87**, 146603 (2001).

[7] Faist, J., Capasso, F., Sirtori, C., Sivco, D. L., Hutchinson, A. L., Hybertsen, M. S., and Cho, A. Y., "Quantum cascade lasers without intersubband population inversion," *Phys. Rev. Lett.* **76**, 411 (1996).

[8] M. F. Pereira, J., "Intervalence transverse-electric mode terahertz lasing without population inversion," *Phys. Rev. B* **78**, 245305 (2008).

[9] Weber, C., Banit, F., Butscher, S., Knorr, A., and Wacker, A., "Theory of the ultrafast nonlinear response of terahertz quantum cascade laser structures," *Appl. Phys. Lett.* **89**, 091112 (2006).

[10] Waldmueller, I., Chow, W., Young, E., and Wanke, M., "Nonequilibrium many-body theory of intersubband lasers," *IEEE Journal of Quantum Electronics* **42**, 292 (2006).

[11] Savić, I., Vukmirović, N., Ikonić, Z., Indjin, D., Kelsall, R. W., Harrison, P., and Milanović, V., "Density matrix theory of transport and gain in quantum cascade lasers in a magnetic field," *Phys. Rev. B* **76**, 165310 (2007).

[12] Callebaut, H. and Hu, Q., "Importance of coherence for electron transport in terahertz quantum cascade lasers," *J. Appl. Phys.* **98**, 104505 (2005).

[13] Weber, C., Wacker, A., and Knorr, A., "Density-matrix theory of the optical dynamics and transport in quantum cascade structures: The role of coherence," arXiv:0811.3736 (2008).

[14] Waldmueller, I., Chow, W., Gin, A., Young, E., and Wanke, M., "Gain without inversion: An approach for THz quantum cascade laser?," *IEEE 20th International Semiconductor Laser Conference, 2006. Conference Digest. 2006*, 41 (2006).

[15] Lee, S.-C. and Wacker, A., "Nonequilibrium Green's function theory for transport and gain properties of quantum cascade structures," *Phys. Rev. B* **66**, 245314 (2002).

[16] Lee, S.-C., Banit, F., Woerner, M., and Wacker, A., "Quantum mechanical wavepacket transport in quantum cascade laser structures," *Phys. Rev. B* **73**, 245320 (2006).

[17] Wacker, A., "Lasers: Coexistence of gain and absorption," *Nature Physics* **3**, 298 (2007).

[18] Terazzi, R., Gresch, T., Giovannini, M., Hoyler, N., Sekine, N., and Faist, J., "Bloch gain in quantum cascade lasers," *Nature Physics* **3**, 329 (2007).

[19] Revin, D. G., Soulby, M. R., Cockburn, J. W., Yang, Q., Manz, C., and Wagner, J., "Dispersive gain and loss in midinfrared quantum cascade laser," *Appl. Phys. Lett.* **92**, 081110 (2008).

[20] Wacker, A., "Gain in quantum cascade lasers and superlattices: A quantum transport theory," *Phys. Rev. B* **66**, 085326 (2002).

[21] Banit, F., Lee, S.-C., Knorr, A., and Wacker, A., "Self-consistent theory of the gain linewidth for quantum cascade lasers," *Appl. Phys. Lett.* **86**, 41108 (2005).

[22] Ando, T., "Line width of inter-subband absorption in inversion layers: Scattering from charged ions," *J. Phys. Soc. of Japan* **54**, 2671 (1985).

[23] Kumar, S., Williams, B. S., Hu, Q., and Reno, J. L., "1.9 THz quantum-cascade lasers with one-well injector," *Appl. Phys. Lett.* **88**, 121123 (2006).

[24] Willenberg, H., Döhler, G. H., and Faist, J., "Intersubband gain in a bloch oscillator and quantum cascade laser," *Phys. Rev. B* **67**, 085315 (2003).

[25] Nelander, R. and Wacker, A., "Temperature dependence of the gain profile for terahertz quantum cascade lasers," *Appl. Phys. Lett.* **92**, 081102 (2008).
[26] Chow, W. W. and Koch, S. W., *Semiconductor - Laser Fundamentals*, Springer, Berlin (1999).
[27] Kumar, S., Williams, B. S., Kohen, S., Hu, Q., and Reno, J. L., "Continuous-wave operation of terahertz quantum cascade lasers above liquid-nitrogen temperature," *Appl. Phys. Lett.* **84**, 2494 (2004).
[28] Haug, H. and Jauho, A.-P., *Quantum Kinetics in Transport and Optics of Semiconductors*, Springer, Berlin (1996).
[29] Wacker, A., "Semiconductor superlattices: A model system for nonlinear transport," *Phys. Rep.* **357**, 1 (2002).